Diffusion and configuration of Li in ZnO

K. E. Knutsen, , K. M. Johansen, , P. T. Neuvonen, , B. G. Svensson, and , and A. Yu. Kuznetsov

Citation: Journal of Applied Physics **113**, 023702 (2013); doi: 10.1063/1.4773829
View online: http://dx.doi.org/10.1063/1.4773829
View Table of Contents: http://aip.scitation.org/toc/jap/113/2
Published by the American Institute of Physics

Diffusion and configuration of Li in ZnO

K. E. Knutsen,[1,a)] K. M. Johansen,[1] P. T. Neuvonen,[1,2] B. G. Svensson,[1] and A. Yu. Kuznetsov[1]
[1]*University of Oslo, Centre for Materials Science and Nanotechnology, N-0318 Oslo, Norway*
[2]*Department of Physics and Astronomy, University of Aarhus, Ny Munkegade 120, 8000 Aarhus, Denmark*

(Received 2 November 2012; accepted 12 December 2012; published online 8 January 2013)

Diffusion of Li into ZnO from an "infinite" surface source under oxygen-rich conditions is studied using secondary ion mass spectrometry. The Li concentration-versus-depth profiles exhibit a distinct and sharp drop, which evolves in position with temperature and time. The sharp drop is associated with an efficient conversion from highly mobile Li-interstitials (Li_i) to practically immobile Li-substitutionals (Li_{Zn}) via a kick-out mechanism. The characteristic concentration level at which Li drops provides a measure of the active donor concentration in the samples at the processing temperature, and gives evidence of residual impurities being responsible for the commonly observed "native" n-type conductivity. These donors are suggested to arise from different impurities, with Al and Si as the prevailing ones in hydrothermal and melt grown material. Further, evidence of electric field effects on Li diffusion profiles is obtained, and they are considered as a main reason for the slow diffusivity obtained in this work (using O-rich conditions) relative to those previously reported in the literature (obtained under Zn-rich conditions). © *2013 American Institute of Physics*. [http://dx.doi.org/10.1063/1.4773829]

I. INTRODUCTION

Hydrothermal (HT) ZnO exhibits high Li content, typically in excess of 2×10^{17} cm^{-3}, as an inevitable consequence of the synthesis method.[1] As suggested initially by Lander[2] and explored further in recent years both experimentally and theoretically,[3–5] lithium in ZnO acts either as an interstitial donor (Li_i^+) or a substitutional acceptor (Li_{Zn}^-). As discussed in Refs. 3–5, a high Li content may cause Fermi level pinning at midgap complicating the efforts of obtaining *p*-type ZnO. Lander performed Li in-diffusion in the presence of zinc vapor to ensure that all Li was in the interstitial donor configuration (Li_i^+). When performed in air, the diffusion was inhibited by the conversion of donors into acceptors (Li_{Zn}^-), resulting in a sharp boundary between the compensated region with high resistivity and the deeper unaffected region. However, the nature of the abrupt resistivity change was not fully understood.

In the present work, we have used secondary ion mass spectrometry (SIMS) to monitor Li diffusion in HT and melt grown (MG) ZnO under O-rich conditions. The obtained diffusion profiles are exploited to elaborate upon the model set forth by Lander.[2] Comparison between the diffusion in HT and MG materials reveals a dependency on the donor concentration present, leading to an estimate of the effective free electron concentration in the respective materials at the diffusion temperature. A two orders of magnitude difference in the effective diffusivity is observed as compared to that under Zn-rich conditions found by Lander,[2] and the difference is attributed to a change in the diffusion pre-factor.

II. EXPERIMENT

As starting material, we used nominally undoped MG ZnO from Cermet, Inc., and HT ZnO bulk samples from SPC Goodwill, with Li contents of $\sim 2 \times 10^{15}$ cm^{-3} and $\sim 2 \times 10^{17}$ cm^{-3}, respectively. The wafers were $10 \times 10 \times 0.5$ mm^3 in size with polished O-face. Li in-diffusion was performed in sealed quartz ampules filled with atmospheric air (O-rich conditions), and the samples were submerged in a Li-containing powder, supplied by Sigma-Aldrich, consisting of Li_2O (97% purity) and ZnO (99.9%) at 1:20 weight ratio.

Two different cooling rates were applied for the Li doping process: either "slow" by cooling in air, or "rapid" by submerging the ampules into water immediately after extraction from the furnace. This cooling rate had a dramatic effect on the measured resistivity, and higher cooling rate resulted in lower resistivity as summarized in Table I. The MG samples were exposed to the ZnO/Li_2O powder mix for 10 min at 500, 525, 550, 575, and 600 °C (labeled A-E), followed by slow cooling. Further, both HT and MG samples (labeled F-M), were treated for 10 min at 450 and 500 °C, followed by rapid cooling. A few of these samples (H, I, L, and M) underwent a pre-treatment at 1500 °C in air for 1 h, followed by mechanical polishing and annealing at 1100 °C in air for 1 h. Such pre-treatment is known to reduce the Li content in HT material to the 10^{15} cm^{-3} range (or below)[1] and also to reduce the hydrogen content.[6,7] The MG samples H and I underwent the same pre-treatment for comparison. In addition, sample N was doped at 600 °C and then rapidly cooled, followed by 10 min sequential annealing in air from 200 °C to 350 °C (50 °C steps), using slow cooling.

Concentration versus depth profiles of Li were monitored by SIMS using a Cameca IMS 7f microanalyzer. A 10 keV O_2^+ ion beam was rastered over a square area with a side length of 100–200 μm. Some of the samples exhibited high electrical resistivity, causing charge buildup during the SIMS measurement, and an electron gun was used for neutralization. In addition to $^7Li^+$, also $^{27}Al^+$, $^{28}Si^+$, $^{56}Fe^+$, and

a)Electronic address: mailto:k.e.knutsen@smn.uio.no.

TABLE I. An overview of Li in-diffusion samples, processing steps, as well as resistivities (ρ) before and after diffusion. In the course of post anneals of sample N, the resistivity evolves toward "HR" meaning "high resistive," i.e., $>10^3\,\Omega\,\mathrm{cm}$. All samples exhibit n-type conductivity.

Sample label	Growth type	Pre-treatment	Temperature [°C]	Time [min]	Cooling rate	Initial ρ [Ω cm]	Resulting ρ [Ω cm]
A-E	MG	No	500–600	10	Slow	~0.7	HR
F	MG	No	450	10	Rapid	0.94	0.81
G	MG	No	500	10	Rapid	0.94	0.98
H	MG	Yes	450	10	Rapid	1.44	2.21
I	MG	Yes	500	10	Rapid	1.44	1.53
J	HT	No	450	10	Rapid	630	1125
K	HT	No	500	10	Rapid	630	1197
L	HT	Yes	450	10	Rapid	0.82	0.90
M	HT	Yes	500	10	Rapid	0.82	1.20
N	HT	No	600	60	Rapid	…	0.1 → HR

$^{70}Zn^+$ ions were monitored, and the impurity signals were calibrated using implanted reference samples. The crater depths were measured using a Dektak 8 stylus profilometer, and a linear relation between sputtering time and depth was assumed. The resistivity was measured at room temperature using a four point probe setup in the course of all processing steps.

III. RESULTS AND DISCUSSION

Fig. 1 shows typical Li diffusion profiles, where the penetration depth increases systematically as a function of temperature. A key feature is a sharp drop when the concentration falls below a certain level. Indirectly, Lander[2] also observed a similar drop (under O-rich conditions) by monitoring the resistivity after different etching durations. The characteristic concentration level where the drop takes place is found to be independent of diffusion temperature and

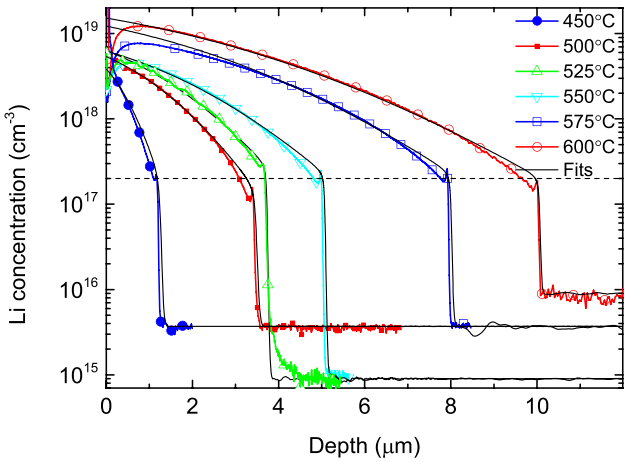

FIG. 1. Li concentration vs. depth profiles in MG ZnO as measured at various temperatures (symbols) and corresponding numerical fits (lines) assuming a kick-out mechanism controlled by the Fermi level position. The dashed line represents a characteristic concentration level ($\sim 2\times10^{17}\,\mathrm{cm}^{-3}$) at which the Li concentration drops in MG ZnO. For HT ZnO, this level is higher ($\sim 5\times10^{17}\,\mathrm{cm}^{-3}$). The baseline level of Li in the bulk, used for the simulations, is taken from the SIMS data and varies somewhat for the different samples.

time, but dependent on the type of material used. For instance, in MG and HT samples, the characteristic concentration level equals typically $\sim 2\times10^{17}\,\mathrm{cm}^{-3}$ and $\sim 5\times10^{17}\,\mathrm{cm}^{-3}$, respectively, as illustrated for the MG samples in Fig. 1. This could possibly be attributed to trap-limited diffusion (TLD),[8] although such an extremely abrupt drop in concentration is not readily accounted for by TLD. Further, the most obvious candidate as a trap for Li_i would be the zinc vacancy (V_{Zn}); however, the concentration of V_{Zn} in similar samples is found to be only $\sim 5\times10^{16}\,\mathrm{cm}^{-3}$, which is about one order of magnitude too low relative to the characteristic level.[9] Hence, V_{Zn} is excluded as a dominant trap for Li and TLD is not regarded as the dominant mechanism. Another option is the model originally proposed by Lander,[2] where Li interstitial donors (Li_i^+) are the mobile species, which convert into significantly less mobile substitutional acceptors (Li_{Zn}^-) and highly mobile Zn interstitials (Zn_i^{2+}) in O-rich conditions through the kick-out mechanism

$$Li_i^+ + Zn_{Zn} \rightarrow Zn_i^{2+} + Li_{Zn}^- . \quad (1)$$

According to Huang *et al.*,[10] such a kick-out mechanism has a barrier of $\geq 1.56\,\mathrm{eV}$

$$E_f(Li_i^+) + E_f(Zn_{Zn}) < E_f(Li_{Zn}{}^-) + E_f(Zn_i^{2+}). \quad (2)$$

Thus, the conversion relies on the efficient removal of Zn_i during the in-diffusion of Li_i. Thomas[11] showed that Zn_i has a higher diffusivity than Li_i in the given temperature range, consistent with recent results by Vines *et al.*,[12] demonstrating a high mobility of Zn_i.

Since Zn_i is rapidly removed, Li_i will efficiently be converted into Li_{Zn} until it balances the background donor concentration. Such an efficient conversion will lead to an abrupt drop in the concentration (see, Fig. 1), as Li_{Zn} is practically immobile at the present temperatures. However, when exceeding the background donor concentration, the kick-out becomes less dominant (E_F moves closer to the middle of the bandgap) and Li_i and Li_{Zn} will coexist in similar concentrations. Thus, the characteristic level at which the concentration of Li changes abruptly corresponds to the background concentration of ionized donors in the material at the diffusion temperature (excluding both Li_i and Zn_i). As mentioned, this background is found to be higher in the HT-material ($5\times10^{17}\mathrm{cm}^{-3}$) than in the MG one ($2\times10^{17}\mathrm{cm}^{-3}$). In an effort to identify these donors, a few samples were subjected to a pretreatment (1500 °C + polishing + 1100 °C), which is known to affect the concentration of both intrinsic defects and residual impurities like H and Li.[6,7,13] However, the effect on the abrupt drop in concentration is relatively small for both MG and HT samples, $\sim 0.3\times10^{17}\,\mathrm{cm}^{-3}$ and $\sim 1\times10^{17}\,\mathrm{cm}^{-3}$, respectively, see Fig. 2. Hence, other donor species than H and intrinsic ones (e.g., V_O) are dominant in this process.

Further, the pretreatment increases the carrier concentration in HT samples due to out-diffusion of Li,[1,14] while the concentration of other impurities (except hydrogen)[6] remains essentially constant. From Refs. 15 and 16, it can be seen that the known donor impurities with a concentration in the

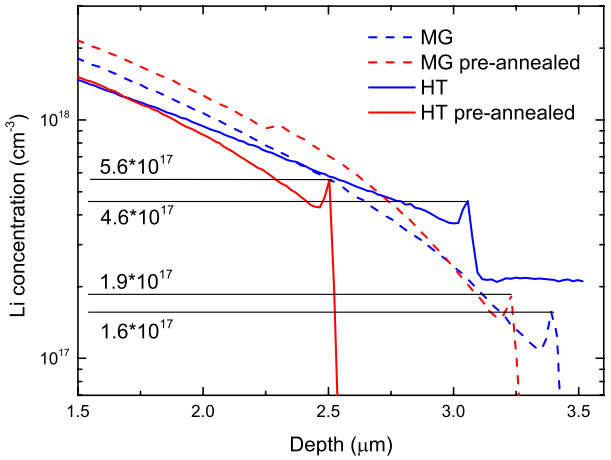

FIG. 2. Details of the level where Li concentration drops in HT and MG samples in-diffused at 500 °C in as-grown and pre-treated samples (specifically samples G, I, K, and M). The same trends holds in samples diffused at 450 °C.

high 10^{16} cm^{-3} to 10^{17} cm^{-3} range, present in HT and MG materials, are Al, Si, Fe, and Ni. Of these, Al, Si, and possibly Fe are considered shallow donors and are likely to contribute to the electron carrier concentration.[17–19] Fig. 3 summarizes the content of Al, Si, and Fe as measured by SIMS in selected samples, in comparison with the background donor concentration estimated from modeling of the experimental data.

Despite an obvious trend of higher purity of MG samples as compared with the HT ones, the contribution from one single element does not agree with the concentration of estimated donors. However, the sum of individual contributions of Al and Si is in closer agreement, indicating that a combination of several donor impurities is responsible for the estimated free electron concentration. Fe content in the present samples is comparable to that of Al and Si as shown in Fig. 3. Note that the total donor concentration is anticipated to be somewhat higher than the carrier concentration, due to compensating acceptors other than Li_{Zn}.

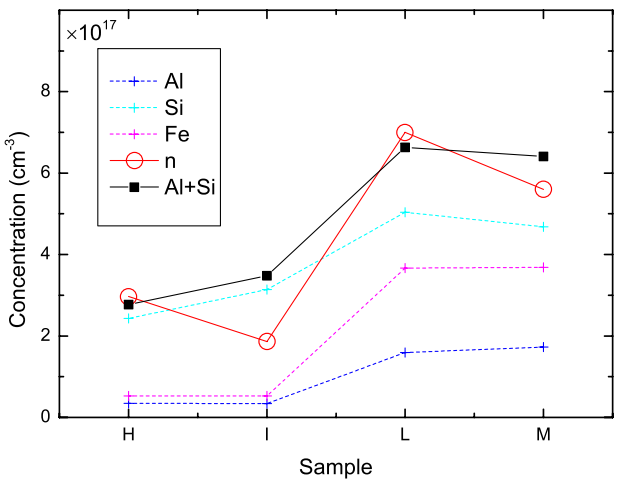

FIG. 3. Impurity contents in selected MG and HT ZnO samples in comparison with the concentration of electrons n before compensation by Li, as deduced from numeric model using Eq. (3).

To compare with the measured profiles of Li and estimate the Li_i diffusivity, we employ the following model:

$$\begin{aligned}\frac{\partial[\mathrm{Li_i}]}{\partial t} &= D_{\mathrm{Li_i}}\frac{\partial^2[\mathrm{Li_i}]}{\partial x^2} - \frac{\partial[\mathrm{Li_{Zn}}]}{\partial t}\\ \frac{\partial[\mathrm{Zn_i}]}{\partial t} &= D_{\mathrm{Zn_i}}\frac{\partial^2[\mathrm{Zn_i}]}{\partial x^2} + \frac{\partial[\mathrm{Li_{Zn}}]}{\partial t}\\ \frac{\partial[\mathrm{Li_{Zn}}]}{\partial t} &= K([\mathrm{Li_i}]\times n) - \nu[\mathrm{Li_{Zn}}]\\ n &= N_d + [\mathrm{Li_i^+}] + 2[\mathrm{Zn_i^{2+}}] - [\mathrm{Li_{Zn}^-}],\end{aligned} \tag{3}$$

where the electron concentration, n, represents the Fermi-level, which is lowered by the reaction in Eq. (1) when Li_i^+ is converted into Li_{Zn}^-. $K = 4\pi R D_{Li_i}$ is the conversion rate coefficient. R is the effective capture radius and D_{Li_i/Zn_i} is the Li/Zn interstitial diffusivity. ν is the rate constant for the reaction $Li_{Zn} \rightarrow Li_i + V_{Zn}$. As boundary condition, the interstitial Li concentration at the sample surface was held constant, $[Li_i(x=0,t)] = const.$, at a given temperature. The fits obtained by employing this model describes the main features of the experimental Li profiles obtained, as illustrated for the MG samples in Fig. 1. An effective capture radius of $R = 8$ nm is estimated, and such a large value is normally indicative of Coulombic attraction between the species involved. The dissociation rate is too low to be determined with any significant accuracy from these data, and is approximated to be zero; the abrupt slope that occurs does not show any temperature dependence, presumably limited by surface roughness evolving during SIMS measurements.

There is one distinct feature that is not accounted for by this model and requires additional consideration. Immediately prior to the drop in the Li concentration-versus-depth profiles, a small but characteristic peak appears, which is always present. This peak occurs at the deep end of the profile where Li_i is converted into Li_{Zn} almost instantly. In addition, preceding this peak, there is a region with lower Li concentration than that predicted by the model, Fig. 1. The abrupt change in effective doping concentration close to the diffusion front will lead to a localized electric field pointing towards the surface, or put another way, an n^-–n junction forms with the associated space charge region and electric field. This electric field leads to a deviation from the profile shape predicted by the model used in Fig. 1, which extends about 1 μm prior to the drop. In lightly doped or highly compensated material, the field can readily extend over such distances at elevated temperatures because of the large Debye length. Furthermore, the extracted values for the Li diffusivity are plotted in Fig. 4 versus the reciprocal absolute temperature, and an activation energy (E_a) and a pre-factor (D_0) of 1.34 ± 0.08 eV and 1.5×10^{-2} cm^2/s are estimated, respectively. These diffusivities are approximately two orders of magnitude lower than those found by Lander (Fig. 4), where the difference arises mainly from a factor of 200 lower D_0 in our case (as illustrated by a parallel line in Fig 4). This indicates that the diffusivity may be highly retarded by the presence of an electric field. Lander used Zn-rich atmosphere to avoid conversion of Li from mobile donors to immobile acceptors, while in our case (O-rich), this

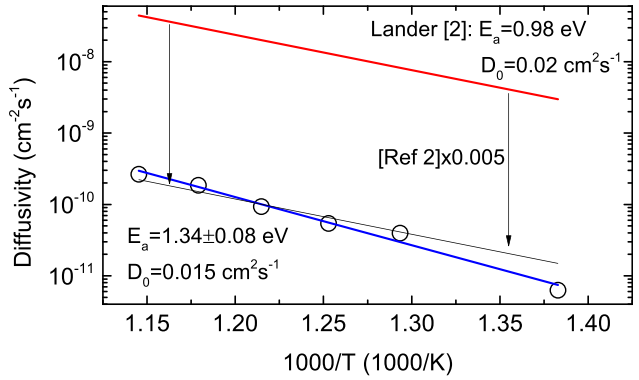

FIG. 4. Arrhenius plot for the effective diffusivity of interstitial Li in MG ZnO. Red line indicates values as reported in Ref. 2, while the black line is the same values reduced by a factor of 200. Note that the estimated error is purely statistical.

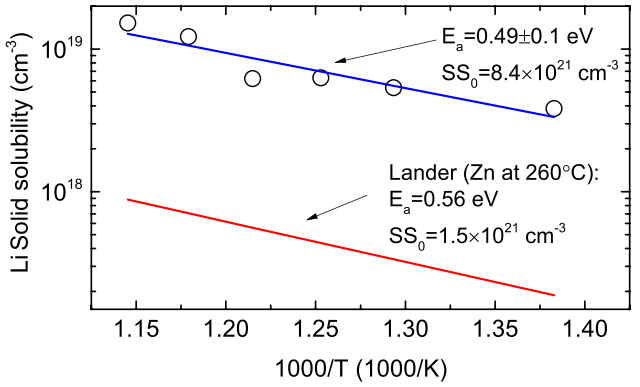

FIG. 6. Arrhenius plot for the solid solubility of Li in MG ZnO. The red line indicates values estimated in Ref. 2.

conversion indeed takes place, resulting in the electric field at the n^-–n junction. In Landers case (Zn-rich conditions), a similar electric field, which points in the opposite direction, may be present due to an n^+–n junction, resulting in an increase in the apparent diffusivity. Hence, the difference in absolute diffusivity values between the two studies may be due to opposite electric fields, which modifies the pre-factor in different directions, but does not affect the activation energy. As such, the intrinsic diffusivity is most likely somewhere in between the two sets of values in Fig. 4.

Fig. 5 shows the resistivity as a function of post-diffusion annealing temperature for sample N (quenched after Li diffusion). The resistivity remains unchanged (~0.1 Ω cm) up to 300 °C, while after 350 °C, it increases by more than three orders of magnitude. This implies that during subsequent anneals in air above 300 °C (or during slow cooling), the ratio $[Li_i]/[Li_{Zn}]$ decreases significantly. This does not necessarily mean a large change in the concentrations of any of the two species if they are fairly similar initially. In fact, the model described by Eq. (3) indicates that $[Li_i]$ is quite similar to $[Li_{Zn}]$ after quenching. SIMS data for quenched samples after post-diffusion annealing at 600 °C, reveal a reduction in the Li concentration attributed to out-diffusion of Li donors. In addition, conversion of Li_i^+ donors to LI_{Zn}^- acceptors are indeed anticipated to reduce the free

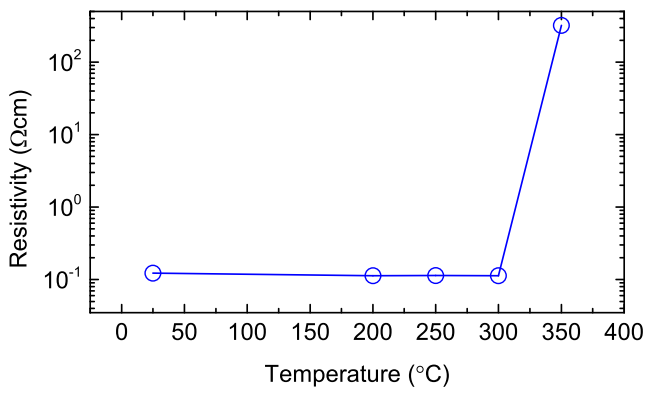

FIG. 5. Resistivity of sample N after sequential post-diffusion anneals at indicated temperatures for 10 min.

electron concentration. In fact, the temperature at which the resistivity increase (350 °C) is in accordance with the barrier calculated by Huang *et al.*[10] (>1.56 eV) for conversion of Li_i to Li_{Zn}.

Assuming a semi-infinite source and no potential barriers or secondary phases at the surface, the intercept of the concentration profiles with the y-axis in Fig. 1 may be used as estimates for the solid solubility of Li in ZnO. In Fig. 6, these values are depicted vs. the inverse absolute temperature, and resulting in an activation energy of the solid solubility of 0.49 eV with a pre-factor of 8.4 $\times 10^{21}$ cm^{-3}. In fact, these values are in close agreement with theoretically obtained values of $1.7 \times 10^{22}\exp(-0.47\text{eV}/\text{kT})\text{cm}^{-3}$, found in a density functional theory study by Bjørheim *et al.*[20] The activation energy is also in close agreement with that reported by Lander,[2] as illustrated in Fig. 6. The difference by about a factor of 5–6 in the pre-factor between the two data sets can be attributed to the experimental methods employed. Lander used resistivity measurements and as such measured the absolute difference between Li_i and Li_{Zn} and not the total Li concentration. SIMS on the other hand unveils the total Li concentration irrespective of atomic configuration.

IV. CONCLUSION

The diffusion of Li in ZnO is found to be dominated by Li_i, which is converted into Li_{Zn} under O-rich conditions by a kick-out mechanism, while trapping free electrons provided by donor impurities. As a result, an n^- layer builds up gradually and at the evolving n^-–n junction a sharp drop in the Li concentration depth profile occurs. The estimated charge carrier concentration at which the drop occurs compares well with the concentration of known ionized donor impurities, thus providing an indication that elements like Al and Si, are responsible for the native n-type conductivity commonly observed in ZnO. The extracted diffusivity is an apparent one, affected by the electric field at the n^-–n junction. This leads to a reduced pre-factor of the diffusion constant, while the activation energy is similar to that previously reported by Lander.[2] Finally, the solubility of Li is deduced to have an activation energy and pre-factor of 0.49 eV and 8.4 $\times 10^{21}$ cm^{-3}, respectively, in close agreement with recent theoretical predictions.[20]

ACKNOWLEDGMENTS

Financial support from the Research Council of Norway provided through the FRINAT project "Understanding ZnO" and FRINATEK project "WEDD" is acknowledged.

[1]E. V. Monakhov, A. Y. Kuznetsov, and B. G. Svensson, J. Phys. D **42**, 153001 (2009).
[2]J. J. Lander, J. Phys. Chem. Solids **15**, 324 (1960).
[3]P. T. Neuvonen, L. Vines, A. Yu. Kuznetsov, B. G. Svensson, X. Du, F. Tuomisto, and A. Hallén, Appl. Phys. Lett. **95**, 242111 (2009).
[4]M. G. Wardle, J. P. Goss, and P. R. Briddon, Phys. Rev. B **71**, 155205 (2005).
[5]C. H. Park, S. B. Zhang, and S. H. Wei, Phys. Rev. B **66**, 073202 (2002).
[6]K. M. Johansen, J. S. Christensen, E. V. Monakhov, A. Yu. Kuznetsov, and B. G. Svensson, Appl. Phys. Lett. **93**, 152109 (2008).
[7]N. H. Nickel and K. Fleischer, Phys. Rev. Lett. **90**, 197402 (2003).
[8]M. S. Janson, A. Hallén, M. K. Linnarsson, and B. G. Svensson, Phys. Rev. B **64**, 195202 (2001).
[9]K. M. Johansen, A. Zubiaga, I. Makkonen, F. Tuomisto, P. T. Neuvonen, K. E. Knutsen, E. V. Monakhov, A. Yu. Kuznetsov, and B. G. Svensson, Phys. Rev. B **83**, 245208 (2011).
[10]G. Huang, C. Wang, and J. Wang, J. Phys.: Condens. Matter **21**, 345802 (2009).
[11]D. G. Thomas, J. Phys. Chem. Solids **3**, 229 (1957).
[12]L. Vines, P. Neuvonen, A. Kuznetsov, J. Wong-Leung, C. Jagadish, and B. Svensson, in *MRS Proceedings* (Cambridge University Press, 2012), Vol. 1394.
[13]F. A. Selim, M. H. Weber, D. Solodovnikov, and K. G. Lynn, Phys. Rev. Lett. **99**, 085502 (2007).
[14]L. Vines, E. V. Monakhov, R. Schifano, W. Mtangi, F. D. Auret, and B. G. Svensson, J. Appl. Phys. **107**, 103707 (2010).
[15]L. Vines, E. V. Monakhov, and B. G. Svensson, Phys. B: Condens. Matter **404**, 4386 (2009).
[16]M. D. McCluskey and S. J. Jokela, Phys. B: Condens. Matter **401–402**, 355 (2007).
[17]R. Schifano, E. V. Monakhov, L. Vines, B. G. Svensson, W. Mtangi, and F. D. Auret, J. Appl. Phys. **106**, 043706 (2009).
[18]J. L. Lyons, A. Janotti, and C. G. Van de Walle, Phys. Rev. B **80**, 205113 (2009).
[19]V. Quemener, L. Vines, E. V. Monakhov, and B. G. Svensson, "Iron related donor defect in ZnO," (unpublished).
[20]T. S. Bjørheim, S. Erdal, K. M. Johansen, K. E. Knutsen, and T. Norby, J. Phys. Chem. C **116**(44), 23764 (2012).